ARTICLE

Received 00th January 20xx,

Accepted 00th January 20xx

DOI: 10.1039/x0xx00000x

Design, synthesis and comparison of water-soluble phthalocyanine/porphyrin analogues on inhibition of $A\beta_{42}$ fibrillization

Weiyuan Xu,[a] Chao Gao,[a] Xinyang Sun, [a] William Chi-Shing Tai,[a] Hong Lok Lung[b] and Ga-lai Law*[a]

The misfolding and fibrillization of β amyloid (Aβ) is a major pathological hallmark of Alzheimer's disease (AD) and creates an important niche for developing targeted probe and drug designs. Phthalocyanine and porphyrin analogues are known to interact with Aβ species and interrupt their aggregation, and in this study we show that by conjugating to small molecules that can function as Aβ aggregation blockers such as curcumin and bexaroten, improved potential drug candidates can be developed. In this work, we investigated porphyrin zinc (ZnPorp) analogues and phthalocyanine zinc (ZnPc) conjugates and compared their inhibitory effects on formation of $A\beta_{42}$ fibrils. We show that probe designs with a good hydrophilic-hydrophobic balance as observed with the ZnPc conjugate analogues are deemed as better inhibitors in modulating $A\beta_{42}$ aggregation.

Introduction

Amyloid plaque deposition is one of the significant pathological hallmark in brains of Alzheimer's disease (AD) patients, and arise due to the abnormal aggregation of excess amyloid β (Aβ) peptides mainly including $A\beta_{40}$ and $A\beta_{42}$. [1-3] $A\beta_{42}$ is more prone to aggregate than $A\beta_{40}$ and its oligomeric species are found to be more toxic to neurons other than fibrils or mature plaques. [2, 4, 5] Aβ over-expression and misfolding are regarded to be one of the important factors for synaptic dysfunction and neurodegeneration. [6] Yet, currently there is no successful therapy for AD treatment, and hence there is an urgent need to evaluate potential therapeutic candidates to alleviate Aβ accumulation as well as to develop potential treatment strategies. [7-9]

Phthalocyanines (Pcs) and porphyrins (Porp) belongs to a class of cyclic tetrapyrrole compounds and they are characterized by a planar aromatic ring system which can display a strong and selective binding with aromatic amino acid residues *via* π-π interactions. These interactions are found to exhibit inhibition on diseases associated with protein aggregation and the induced toxicity. Examples of such, includes;- prion protein (PrP), [10-12] alpha-synuclein (αS), [13, 14] tau [15, 16] and Aβ self-assembly. [17-19] As a class of widely investigated photosensitizers in photodynamic therapy, Pcs and porphyrins can contribute to low dark toxicity and afford easy modifications by synthetic methods. [20-23] Particularly, water soluble Pc tetrasulfonate (PcTS) analogues have been shown to reduce toxic Aβ oligomers by aromatic and hydrophobic interactions, [19, 24] and its performance of interrupting fibrillization was improved by coordinating with Zn (II) ion. [17] 5,10,15,20-tetrakis(N-methyl-4-pyridyl)-porphyrin (TMPyP4) is a planar and water soluble cationic porphyrin which was shown to be able to inhibit the formation of both Aβ oligomers and fibrils, with IC_{50} at 0.6 and 0.43 μM respectively, meanwhile alleviating the cytotoxicity induced by Aβ species. [25]

Many strategies have been investigated in the field of blocking Aβ aggregation by designing Pc and porphyrin analogues of higher affinities to Aβ peptides. The hydrophobic KLVFF region of $A\beta_{42}$ is regarded to be responsible for Aβ aggregation, [26] and it was found to prevent aggregation by binding to the full length of Aβ. [27] By linking KLVFF segment to porphyrin analogues higher affinities of porphyrins to bind Aβ species were acquired [28, 29] while degradation of Aβ aggregates and alleviation of cell toxicity were achieved after light irradiation. [28] In work by Shatera et al. water soluble

[a] *State Key Laboratory of Chemical Biology and Drug Discovery, Department of Applied Biology and Chemical Technology, The Hong Kong Polytechnic University, Hung Hom, Kowloon, Hong Kong SAR, PR China.*

[b] *Department of Chemistry, Hong Kong Baptist University, Kowloon, Hong Kong SAR, P.R China*

E-mail: ga-lai.law@polyu.edu.hk

Electronic Supplementary Information (ESI) available: See DOI: 10.1039/x0xx00000x

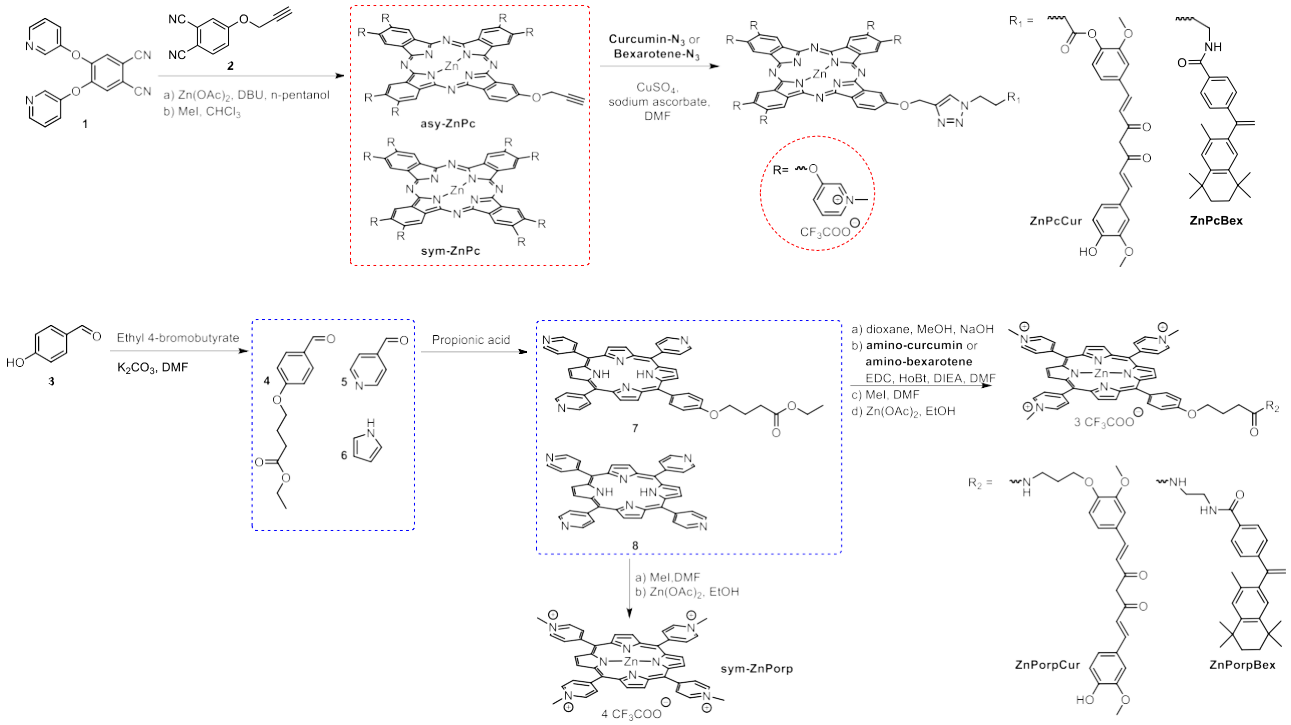

Scheme 1. Synthesis of water soluble ZnPc/porphyrin analogues and the conjugates with curcumin and bexarotene, *i.e.* sym-ZnPc, ZnPcCur ZnPcBex, sym-ZnPorp, ZnPorpCur and ZnPorpBex respectively.

$ZnPc(COONa)_8$ decorated with carboxylic groups was able to both inhibit Aβ fibril formation and destabilize pre-formed fibrils. [18] Further studies by Qichen et al. also showed that by introducing thymine groups to a ZnPc , they developed a compound that had strong affinity to iron (III) and aluminum (III). This is important as abnormally high levels of metal ions are found in brains of AD patients Their work showed that after photoexcitation, protofibrils degradation and neuron protection effects were observed. [30]

As many small molecules are found to be potent in developing AD therapeutic, in our work we focused on using small bioactive molecules as targeting vectors for the design of our probes. In the work we design a probe with a bioactive natural product, curcumin which is shown in literature to bind specially to Aβ plaques and to be capable of chelating metals such as copper and iron. [31, 32] Curcumin interacts with side chains of bolded residues of HQKLVFF sequence length *via* non-covalent contacts like hydrophobic and hydrogen bonding interactions. [33] The methoxy and/or hydroxy groups of curcumin play a significant role in its interaction with the $Aβ_{42}$ fibrils as well. [34] These actions can disrupt the formation of β-sheet structure that is responsible for Aβ aggregation. Unfortunately, although it shows many beneficial properties, it is limited by its poor bioavailability. Bexarotene as a retinoid X receptor (RXR) agonist has been proved with potential of soluble Aβ clearance as well as Aβ plaque clearance in a short time *in vivo*. [35] Although it could hardly reduce plaque burden upon interaction with Aβ plaque, bexarotene was shown to delay fibrils growth. [36]

In this study, attempts have been done to improve the performance of both porphyrins and Pcs in regulating the aggregation process of $Aβ_{42}$ peptide by adopting a conjugating strategy with small inhibiting molecules. Hydrophilic-modified Pc and porphyrin were conjugated to small molecules that had Aβ inhibition properties such as curcumin and bexarotene respectively. The given Pc conjugates were compared in terms of inhibiting $Aβ_{42}$ fibrillization by using thioflavin t (ThT) assay, circular dichroism (CD), western blot and transmission electron microscopy (TEM). We also compared these compounds to a symmetrical ZnPc (sym-ZnPc) which has no conjugation to serve as a control. In this work, our ZnPc conjugates showed improved inhibition on $Aβ_{42}$ fibrillisation, which is attributed to the transformation of $Aβ_{42}$ species from the soluble state to the insoluble form. In our work, we also compared this to the ZnPorp analogues conjugated to the curcumin or bexarotene molecule. Comparative studies were performed by CD spectroscopy, western blot and TEM analysis, which showed that these compounds were less effective in the anti-fibrillization of $Aβ_{42}$.

Results and discussion

Design and synthesis of the Zn Pc and Porphyrin compounds

Interaction of inhibitors with disease related peptides is a common strategy for creating an inhibitory process, and apart from the aromatic and hydrophobic interactions, electrostatic interactions between the charged groups of inhibitors and peptide residues can contribute to the stability of the formed complexes. [13, 19] On the other hand, it is known that metal coordination to the core of the tetrapyrroles can strongly regulate molecular interactions due to residual charge or coordination geometry preferences. [19] In our work, cationic Pc and porphyrin analogues were designed by introducing quaternized pyridyls to the ring while the tetrapyrrole core was coordinated with Zn (II) for better interaction affinities as shown in Scheme 1. The synthesis of ZnPc analogues started with phthalonitriles **1** and **2** catalyzed by 1,8-diazabicyclo(5.4.0)undec-7-ene (DBU) in n-pentanol as shown in Scheme 1. The harvested ZnPc mixture was reacted with iodomethane and then extracted with water before separation using reverse phase high performance liquid chromatography (HPLC). Two main products were collected as sym-ZnPc and asy-ZnPc, and click reaction was adopted for bridging asy-ZnPc to small molecules, *i.e.* curcumin-N_3 and bexarotene-N_3 respectively, the synthetic procedures are given in Scheme S1 (supporting information), to give the final compounds ZnPcCur and ZnPcBex.

4-Hydroxybenzaldehyde, 4-pyridinecarboxaldehyde and pyrrole were selected as building blocks for the porphyrin analogues, while ethyl 4-bromobutyrate was reacted with 4-hydroxybenzaldehyde (compound **3**) to give compound **4** in advance according to reported procedures [37] as given in Scheme 1. Afterwards, porphyrin **7** and **8** were acquired by refluxing compound **4**, 4-pyridinecarboxaldehyde and pyrrole in a molar ratio of 1:3:4 in propionic acid. The Boc-amino-curcumin and Boc-amino-bexarotene were synthesized (Scheme S1), and afterwards following a sequence of deprotection, conjugation, hydrophilic modification and metal chelation, metallic porphyrin-curcumin/bexarotene conjugates were given as the final compounds (*i.e.* ZnPorp-Cur and ZnPorp-Bex). Metal chelation was set as the final step because transition metals can be easily complexed to the core of tetrapyrrole compounds at mild condition. [38-40] The final products of porphyrin and Pc analogues were acquired after HPLC separation and then freeze-dried, and before usage the content of each compound was determined according to levels of metal determined by using inductively coupled plasma-optical emission spectrometry (ICP-OES). All the compounds where possible are characterized by methods such as electrospray ionization mass spectrometry (ESI-MS), ^{1}H and ^{13}C nuclear magnetic resonance (NMR).

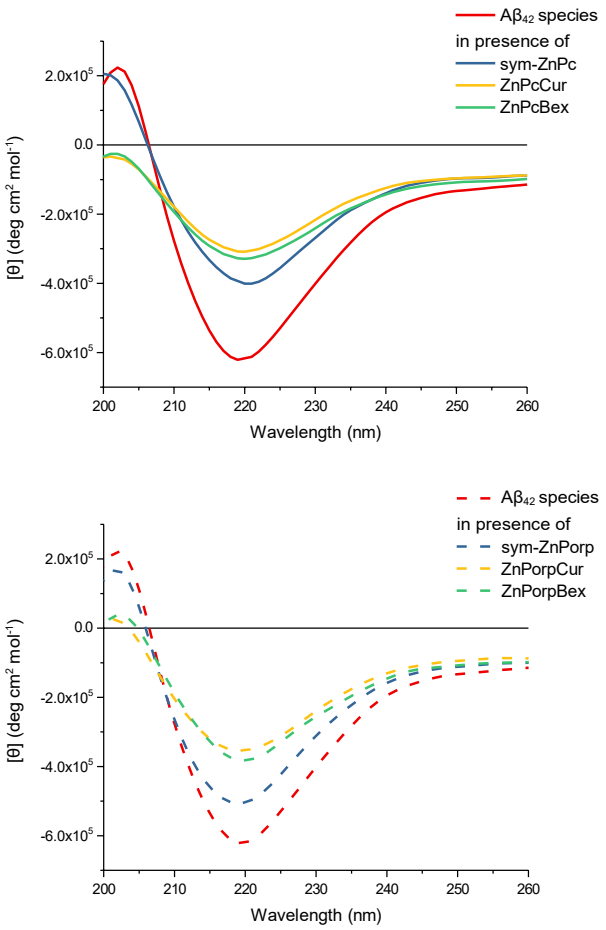

Figure 1. CD spectra of incubated Aβ$_{42}$ species with ZnPc analogues (upper) or ZnPorp analogues (bottom).

Aβ fibrillisation studies

In order to examine the interaction of our probes with the Aβ fibrils, we used many different characterisation techniques. Aβ peptide usually has a native unfolded state which can be slowly transformed into a partially folded state, called β-sheets. In the process of fibrillization, the cooperative folding and assembly of macrocyclic β-sheet peptide can be examined by CD, where a characteristic pattern of β-sheet conformation with absorption minima at around 218 nm are usually observed. [41, 42] In this case, the anti-aggregation effects of our probes, for both ZnPc and porphyrin analogues; were examined by CD spectra directly after incubation. The results are given in Figure 1. From the CD spectra, it is observed that Aβ$_{42}$ monomers after incubation in the absence of inhibitors will exhibit

an intensive negative band at around 220 nm, which indicates the formation of β-sheet structures after fibrillization. However, in the presence of various ZnPc analogues the negative bands are shown to decrease to different extents, which shows that ZnPc compounds can modulate the formation of Aβ secondary structures. The inhibitory effects of ZnPorp analogues are found to be less effective compared to the ZnPc counterparts as indicated by the intensities of CD bands (dash lines) of the Aβ species after incubation. This is reflected quite clearly by comparing the control compounds of the sym-ZnPc and sym-ZnPorp, which indicates that a Pc macrocycle has higher potential of affecting the peptide structure transformation. The linkage of a small molecules such as the curcumin or bexarotene onto the ZnPc/porphyrin ring also induced more inhibition onto the Aβ fibrillization when compared to the sym-ZnPc/sym-ZnPorp, as the conjugates combined the anti-aggregation behaviour of both macrocycles and small molecules.

ThT assay studies

ThT assay is a commonly used method for the identification and qualification of amyloid fibrils *in vitro* when examining misfolding and self-aggregation of proteins in neurodegenerative diseases such as AD. [43, 44] The inhibition potentials of ZnPc analogues on $A\beta_{42}$ fibrillization were compared according to the fluorescence intensity variations of an exogenous ThT assay. Therefore, according to the results in Figure S1A (supporting information), ThT alone has negligible fluorescence but ThT co-incubated with preformed $A\beta_{42}$ fibrils has the highest emission peaked at around 485 nm due to the binding induced fluorescence enhancement. However, in the presence of 10 μM of ZnPcCur or ZnPcBex, the ThT fluorescence emissions were found weak compared to that of the sym-ZnPc at the same concentration (10 μM) which almost accounted for half of the ThT fluorescence intensity of the $A\beta_{42}$ only (control group). These results indicate that the inhibition of sym-ZnPc on fibrillization was not as effective as ZnPc conjugates.

However, inconsistent results were found for Aβ species after incubation with ZnPorp analogues between their ThT emissions and CD spectra. In Figure S1B, minimum ThT fluorescence indicated total inhibition by ZnPorp analogues on Aβ fibrillization, which is in conflict with their CD results in Figure 1 where presence of Aβ fibrils of high levels after incubation was suggested. This phenomenon may be due to the quenching effect on ThT fluorescence by exogenous porphyrin compounds due to their strong absorptive properties at the

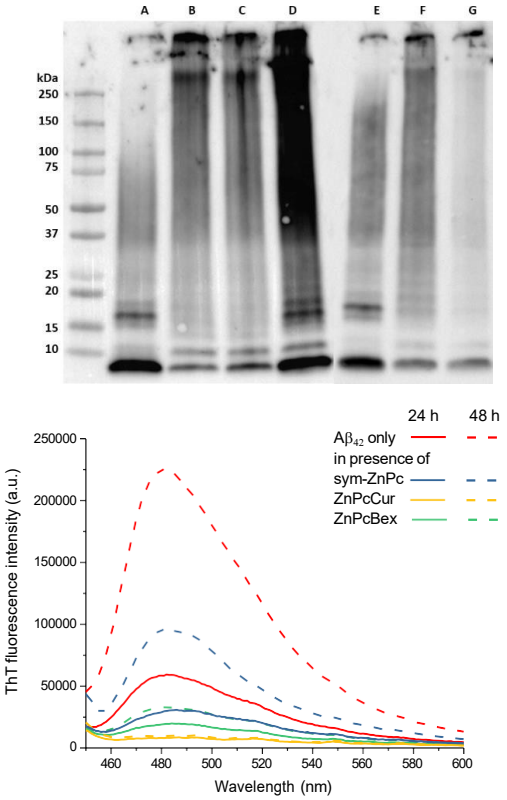

Figure 2. Incubation results of $A\beta_{42}$ peptide in presence of ZnPc/porphyrin compounds. (Upper) Western blot analysis of incubated $A\beta_{42}$ peptide after 48 hours in presence of various compounds, *i.e.* A) $A\beta_{42}$ only, B) sym-ZnPc, C) ZnPcCur, D) ZnPcBex, E) sym-ZnPorp, F) ZnPorpCur, G) ZnPorpBex. (Bottom) ThT emission of groups after incubation with ZnPc analogues for 24 and 48 hours respectively.

excitation wavelength of ThT (at around 440 nm). [43] Besides, porphyrin analogues was found to compete with ThT for the binding sites of Aβ species, [45] which might sacrifice the fluorescence response of ThT. Therefore, the fluorescence emission of ThT is not applicable to reflect the fibrillization extents of Aβ species when incubated with ZnPorp analogues.

To further investigate the microenvironments of Aβ species after incubation, 8-anilino-1-naphthalenesulfonate (ANS) was adopted as an indicator for the degree of hydrophobicity of the incubated Aβ species, as it can bind to hydrophobic patches of the surfaces of solvent-exposed protein aggregates, thus resulting in enhancements in fluorescence emission intensity. [2, 18] The results in Figure S1C show that the fluorescence of ANS incubated with preformed Aβ aggregates increased compared to that of ANS only, while groups of Aβ species in presence of various ZnPc compounds had lower ANS fluorescence intensities following a sequence of sym-ZnPc, ZnPcCur and ZnPcBex. It is supposed that the hydrophobicity of the incubated

Aβ peptides can be controlled due to hydrophobic interactions between ZnPc analogues and Aβ species, where the ANS molecules had less sites to occupy, resulting in their low fluorescence emissions.

Western blotting analysis

Gel electrophoresis/Western blot has been widely used for visualizing the size distribution of Aβ species after incubation. [46-48] With western blotting we were able to show that the ZnPc/porphyrin analogues were found to accelerate the transformation of soluble Aβ species into insoluble forms to different extents as shown by gel analysis in Figure S2. At 10uM, the quenching of fluorescence of ZnPc analogues was observed in the incubation study with $A\beta_{42}$ monomers in Figure S3, this quenching is also known and typical for ZnPorp compounds. [29] This phenomenon arises due to the exogenous compounds inducing aggregation of peptide, however is not consistent with earlier studies which reported that Pc analogues can transform oligomeric Aβ species into large insoluble forms. [24] To understand this process better, we further compared the ZnPc and ZnPorp analogues in this dynamic process at much lower concentrations to avoid the aggregation effect. The compounds concentration was lowered to 1 μM and the compositions were further analysed after 24 and 48 hours of incubation respectively by staining with polyclonal Aβ antibodies. After 24 hours of incubation for the ZnPc analogues, there were similar levels of monomers for ZnPc compounds, but differences were witnessed in their amounts of large oligomers and fibrils as shown in Figure S2, *i.e.* ZnPcBex had more abundant large size oligomers and fibrils among the ZnPc analogues (lane D); the incubated $A\beta_{42}$ (lane A) contained fewer soluble oligomers higher than 75 kiloDalton (kDa). In contrast, ZnPorp analogues were found to promote the formation of Aβ aggregates, with fewer monomers and more protofibrils found in Figure S2 (lane E, F and G).

Obvious clearance of soluble Aβ species was recorded after another 24 hours of incubation for each lane in Figure 2. Relative high amount of monomer residues was observed from the lane of $A\beta_{42}$ and the lane of ZnPcBex, but $A\beta_{42}$ without adding any other compound had the fewest soluble oligomers among the five lanes. Compared to the other lanes, the lane of ZnPcBex had the highest level of soluble oligomers of larger size above 37 kDa, which indicates ZnPcBex could stabilize these soluble species and delay their growth to larger and insoluble pieces. In contrast, the lanes of sym-ZnPc and ZnPcCur were similar, which had the lowest proportions of monomer since most of the species were expected to be transferred into insoluble forms. However, fewer oligomers can be found in the lanes of samples incubated with ZnPorp analogues (lanes E-G, Figure 2), and this phenomenon also indicated that ZnPorp compounds were more capable of transforming Aβ monomers into insoluble species, compared to ZnPc analogues.

ThT fluorescence emissions were then recorded for evaluating the extents of fibrillization after 24 and 48 hours of incubation with ZnPc analogues as shown in Figure 2. The emission intensity of $A\beta_{42}$ alone was the highest for each incubation slot and it was found to increase by more than 4 folds from 24 to 48 hours of incubation. Obvious enhancement of fluorescence intensity was recorded as well in presence of sym-ZnPc, which indicated its less effective anti-aggregation potential, while ZnPcCur and ZnPcBex showed better inhibition results, as indicated by the minimum increases of ThT fluorescence over incubation. Both western blot analysis and ThT assay suggest that ZnPc conjugates effectively avoided the formation of β-sheet structure, although most of peptides were transferred into insoluble species.

TEM analysis

As large and insoluble $A\beta_{42}$ species can hardly be analyzed using western blotting, transmission electron microscopy (TEM) was adopted to view the morphological states of $A\beta_{42}$ species after incubation in order to provide a more complete picture of the extent and pathways of aggregation. [47, 49] Firstly, in the absence of any compounds, $A\beta_{42}$ grew into classic fibrils as shown in Figure 3G. In the presence of sym-ZnPc, long fibrillar species were no longer observed, instead, clusters formed by shorter fibrillar structures were seen in Figure 3A. In the presence of ZnPc conjugates, classic fibrillar structures were also not found (Figure 3C and 3E). The Aβ species observed were disordered and random in both size and shape, which confirms the inhibition of the Aβ aggregation into fibrils and caused transformation into large and insoluble species due to the presence of the ZnPcCur and ZnPcBex compounds. In contrast, this effect was less prominent with the ZnPorp analogues which was also confirmed by TEM images in Figure 3B, D and F, where Aβ fibrils could still be observed, which is consistent with the CD results.

Overall, the sizes of fibrils grown in the presence of ZnPorp compounds were larger but shorter than for the control compound

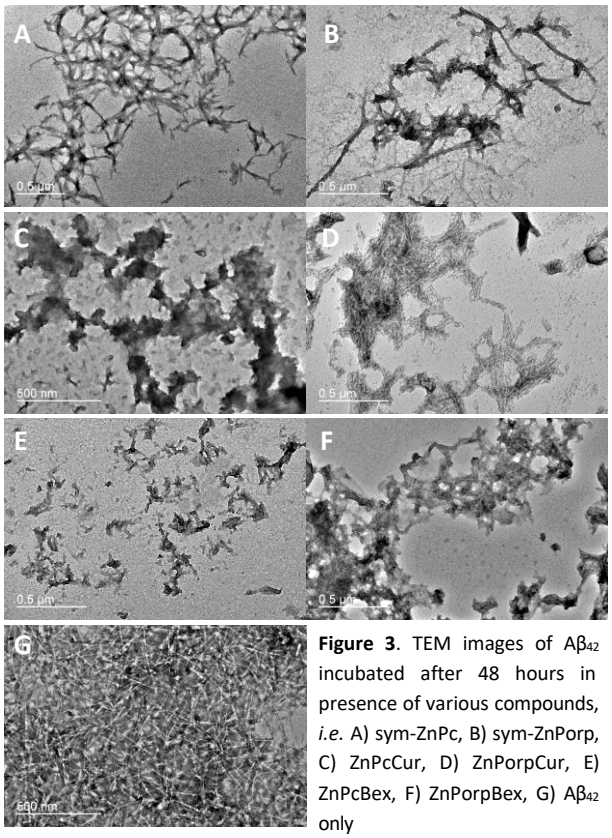

Figure 3. TEM images of $A\beta_{42}$ incubated after 48 hours in presence of various compounds, *i.e.* A) sym-ZnPc, B) sym-ZnPorp, C) ZnPcCur, D) ZnPorpCur, E) ZnPcBex, F) ZnPorpBex, G) $A\beta_{42}$ only

(Figure 3G), suggesting that ZnPorp compounds may work as seeds to accelerate the fibrillization.

The anti-fibrillization potentials of the investigated compounds can be quantified with the aid of indicators, such as thioflavin S (ThS) [15, 16] and ThT. [28] The fluorescent intensities of indicators were used to determine the aggregation extents as a function of the concentration of the ZnPc inhibitors.

The simulated dose dependent curves of 24 hours of incubation results are listed in Figure S4. The half maximal inhibitory concentrations (IC_{50}) were estimated and listed in Table 1. The IC_{50} for sym-ZnPc was the highest, at 1.92 μM, which is around 10 folds of that of ZnPcCur (0.18 μM), while the half inhibition concentration of ZnPcBex were found at 0.27 μM.

Further incubation was continued for another 24 hours to examine the long-term inhibition effects, and the nonlinear fitting curves are given in Figure S5. Obvious increase of half inhibition concentration was observed for the sym-ZnPc from 1.92 to 3.03 μM, this is around 50 %, compared to the first 24 hours of the IC_{50}, indicating sym-ZnPc could not totally inhibit the fibrillization progress. Only minor changes of half inhibition levels were witnessed for the other ZnPc conjugates (Table 1), and the IC_{50} after 48 hours of incubation were found at 0.12 and 0.23 μM for ZnPcCur and ZnPcBex, respectively.

Table 1. Half inhibition levels (IC_{50}) of ZnPc analogues on $A\beta_{42}$ fibrillization.

Compounds	IC_{50}/24 h (μM)	IC_{50}/48 h (μM)
sym-ZnPc	1.92	3.03
ZnPcCur	0.18	0.12
ZnPcBex	0.27	0.23

This result indicates that ZnPc conjugates could totally inhibit $A\beta_{42}$ fibrillization and inactivate the self-assembly of $A\beta_{42}$.

In our study, after conjugating to small molecules, including curcumin or bexarotene, ZnPc conjugates containing 6 positively charged pyridyl groups showed more than 10 folds of improvements of inhibition potentials in contrast to the sym-ZnPc. Curcumin has direct anti-aggregation effects on Aβ species because of its binding to the hydrophobic microenvironment including multiple hydrophobic residues such as phenylalanine to the core fragment (KLVFF) of $A\beta_{40/42}$ peptide. [50] According to Porat et al.'s study, the IC_{50} of curcumin was found as low as 0.63 μM, [51] which is similar to that of TMPyP4 where an IC_{50} of 0.60 μM was determined. [25] In theory, the conjugated small molecules provide extra binding sites for Aβ species; small molecules have intrinsic hydrophobicity, which transfers the ZnPc conjugates to be amphiphilic molecules. This may be responsible for the effective and irreversible inhibitory effects of ZnPc conjugates as shown from the results of ThT assay.

MTT studies

The cytotoxicity of ZnPc/porphyrin analogues was compared in HeLa cells and the results are provided in Figure 4.

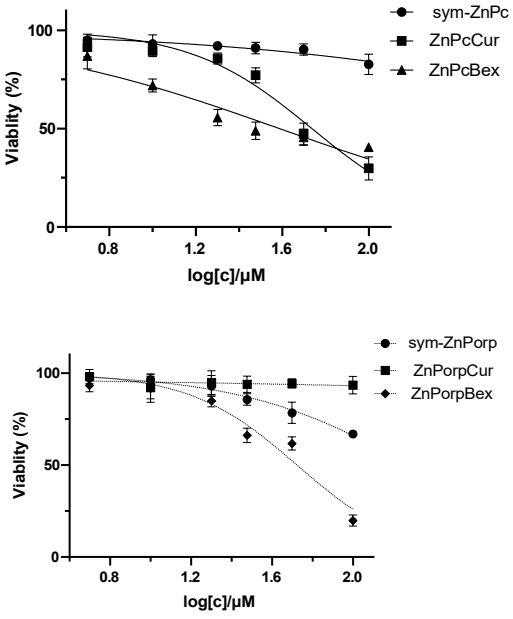

Figure 4. The cytotoxicity of ZnPc/porphyrin analogues on HeLa cell investigated by MTT assay.

Up to 100 µM, there was no obvious toxicity found for sym-ZnPc and ZnPorpCur, while relatively low viability of cells was observed when treated with ZnPcCur, ZnPcBex and ZnPorpBex, with IC_{50} simulated at 55, 39 and 53 µM respectively. From the dose dependent cell survival curves in Figure 4, when applied at low concentrations such as 10 µM, the viabilities were relatively high, which indicates the high feasibility of these compounds for application in biological systems.

Conclusion

Compounds that can inhibit of Aβ fibrillization is important as it can help delay the pathway in AD and perhaps serve as a potential therapeutic or drug candidate. However most affective biological small molecules have bioavailability issues or suffers from poor water solubility, which limits their value in bioapplications. In our work, we have introduced hydrophilic modifications to improve the water solubility and to reduce the tendency of self-aggregation. By conjugating ZnPc/porphyrin to small molecules, including curcumin and bexarotene, ideal candidates for blocking fibrillization were acquired with high sensitivity. Their anti-aggregation performances were examined by using ThT assay, CD spectra, western blotting and TEM. Our results showed that with the aid of selective small molecules, the anti-fibrillization performances of ZnPc analogues can be highly improved. For both ZnPc and ZnPorp analogues, these could assist to transform amyloid species into insoluble species, however the ZnPorp compounds were not able to fully inhibit the fibrillization progress, which indicates that the Pc macrocycle is more effective than the porphyrin ring. Furthermore, the small molecules conjugated with the ZnPc allows these analogues to be more sensitive and effective as inhibitors on fibrillization. Overall, in our comparative studies of the two classes of tetrapyrroles which are known to show anti-aggregation effects to Aβ species, ZnPc conjugates was found in this study to show better performance than porphyrins in controlling Aβ fibrillization. We postulate that this may be due to the better hydrophilic-hydrophobic balance in our designed structure. The conjugation strategy with the selective small biological compounds also shows an ideal approach for developing candidates for further application in AD therapeutics and developing probes for diagnostics.

Experimental

Materials and methods

$Aβ_{42}$ peptide (> 95%) was purchased from abcam (Hong Kong, China). All the chemicals and solvents were purchased as ACS grade and used directly without further purification. 1,1,1,3,3,3-Hexafluoro-2-propanol (HFIP, > 99%), thioflavin T (ThT, Calbiochem) and 8-anilino-1-naphthalene-sulfonic acid (ANS, > 97%) were provided by Sigma-Aldrich. The electrophoresis was run on 4-15% Mini-PROTEAN TGX gel using a Bio-Rad Mini-PROTEAN tetra vertical electrophoresis cell. Polyclonal Aβ antibody was acquired from Cell Signaling (Hong Kong, China) for western blot analysis. The purification of the Pc/porphyrin analogues was conducted on a Waters semi-preparative HPLC system equipped with 2535 Quaternary gradient solvent pump, 2707 Autosampler, 2998 Photodiode array detector and a Waters C18 Column (250 × 19 mm). Liquid chromatography-mass spectrometry was performed using a Waters ACQUITY H-Class UPLC with QDa mass detector. ^1H and ^{13}C NMR spectra were recorded on a Bruker Ultrashield 400 Plus NMR spectrometer (at 400 MHz and 100 MHz, respectively).

Sym-ZnPc and asy-ZnPc

Phthalonitrile **2** (100 mg, 0.55 mmol), phthalonitrile **1** (690 mg, 2.20 mmol) and $Zn(OAc)_2$ (302 mg, 1.65 mmol) were mixed together with 10 mL n-pentanol. The system was firstly heated to 100 °C and stirred for 30 min, and afterwards 250 mg (1.65 mmol) DBU was added and the solution was heated to 140 °C overnight. After that, reaction mixture was added dropwise into n-hexane while constant stirring, and the solid was filtered and then washed with DCM and diethyl ether. After drying, crude products were mixed with 2 mL MeI and stirred for 24 h at 40 °C. The given products were purified by reverse phase HPLC to give **asy-ZnPc**. ^1H NMR (400 MHz, DMSO-d_6) δ (ppm): 3.78 (1H, t, J = 2.4 Hz), 4.42 (12H, s), 4.45 (6H, s), 5.35 (2H, d, J = 2.4 Hz), 7.90 (1H, dd, J = 2.28 Hz, J = 8.34 Hz), 8.25 (6H, m), 8.65 (6H, m), 8.96 (6H, m), 9.27 (1H, d, J = 8.36 Hz), 9.33 (6H, m), 9.40 (3H, m), 9.45 (1H, s), 9.49 (1H, s). ^{13}C NMR (100 MHz, DMSO-d_6) δ (ppm): 48.77, 48.80, 57.05, 79.40, 79.60, 108.21, 116.75, 117.11, 119.28, 124.61, 129.45, 132.42, 133.37, 133.47, 133.88, 136.39, 136.47, 136.59, 136.77, 136.82, 136.85, 136.96, 137.02, 137.07, 140.96, 141.76, 141.91, 146.88, 146.94, 147.07, 147.43, 151.58, 151.89, 152.41, 153.08, 153.67, 155.25, 155.86, 156.23, 156.43, 156.47, 156.51, 160.42. ESI-MS (*m/z*): $[M+4CF_3COO]^{2+}$ calcd. for $C_{79}H_{54}F_{12}N_{14}O_{15}Zn^{2+}$ 865.15; found 866.00.

Sym-ZnPc was collected from the HPLC trials as well. ^1H NMR (400 MHz, DMSO-d_6) δ (ppm): 4.48 (24 H, s), 8.28 (10H, m), 8.71 (10H, d, J = 8.04 Hz), 9.01 (10H, d, J = 6.04 Hz), 9.40 (16H, s). ^{13}C NMR (100 MHz,

DMSO-d_6) δ (ppm): 48.74, 116.91, 129.44, 133.49, 136.57, 137.10, 141.81, 147.18, 153.04, 156.45, 158.16, 158.51, 158.85, 159.20. ESI-MS (*m/z*): $[M+5CF_3COO]^{3+}$ calcd. for $C_{90}H_{64}F_{15}N_{16}O_{18}Zn^{3+}$ 668.45; found 668.80.

ZnPc conjugates with curcumin or bexarotene

ZnPcCur. Asy-ZnPc (58 mg, 0.03 mmol) was mixed with curcumin-N_3 (14 mg, 0.03 mmol), sodium ascorbate (6 mg, 0.03 mmol) and copper sulfate (5 mg, 0.02 mmol) in 3 mL DMF, and then stirred overnight at room temperature, after which the reaction mixture was separated by HPLC to give ZnPcCur. ^{1}H NMR (400 MHz, DMSO-d_6) δ (ppm): 3.76 (3H, s), 3.80 (3H, s), 4.43 (18H, m), 4.83 (2H, t, J = 6.44 Hz), 5.73 (2H, s), 5.87 (1H, s), 6.65 (1H, d, J = 15.84 Hz), 6.71 (1H, d, J = 15.88 Hz), 6.82 (1H, d, J = 8.16 Hz), 7.02 (1H, d, J = 8.12 Hz), 7.11 (1H, s), 7.13 (1H, d, J = 1.8Hz), 7.25 (1H, d, J = 1.8 Hz), 7.34 (1H, s), 7.36 (1H, d, J = 15.76 Hz), 7.50 (1H, d, J = 15.76 Hz), 7.95 (1H, dd, J = 2.28 Hz, J = 8.36 Hz), 8.24 (6H, m), 8.52 (1H, s), 8.64 (6H, m), 8.95 (6H, m), 9.05 (1H, d, J = 2.16 Hz), 9.31 (7H, m), 9.38 (4H, m), 9.45 (1H, s), 9.49 (1H, s), 9.77 (1H, s). ^{13}C NMR (100 MHz, DMSO-d_6) δ (ppm): 19.98, 30.89, 32.66, 32.94, 55.89, 101.47, 101.76, 109.77, 111.44, 114.91, 120.97, 121.08, 121.78, 123.03, 123.20, 124.30, 127.57, 134.00, 134.13, 139.39, 139.96, 141.16, 146.87, 148.06, 151.34, 170.79, 181.83, 183.11, 184.52, 207.11. ESI-MS (*m/z*): $[M+2CF_3COO]^{4+}$ calcd. for $C_{99}H_{77}F_6N_{17}O_{18}Zn^{4+}$ 492.37; found 492.53.

The synthesis of ZnPcBex adopted similar procedures and their structure characterization is listed as following,

ZnPcBex. ^{1}H NMR (400 MHz, DMSO-d_6) δ (ppm): 1.21 (6H, s), 1.24 (6H, s), 1.64 (4H, s), 1.90 (3H, s), 2.17 (2H, t, J = 6.88 Hz), 4.42 (18H, m), 4.53 (2H, t, J = 6.96 Hz), 5.23 (1H, s), 5.69 (2H, s), 6.31 (1H, s), 5.87 (1H, s), 7.05 (1H, s), 7.14 (1H, s), 7.30 (2H, d, J = 8.16 Hz), 7.80 (2H, d, J = 8.36 Hz), 7.94 (1H, dd, J = 8.3 Hz, J = 2.4 Hz), 8.51 (1H, s), 8.63 (7H, m), 8.95 (6H, m), 9.06 (1H, d, 2.24 Hz), 9.32 (7H, m), 9.41 (3H, s), 9.46 (1H, s), 9.52 (1H, s). ^{13}C NMR (100 MHz, DMSO-d_6) δ (ppm): 19.95, 30.43, 32.07, 32.11, 33.95, 34.09, 35.10, 37.08, 48.07, 48.77, 62.78, 116.70, 117.03, 125.48, 126.45, 127.73, 127.96, 128.30, 129.46, 132.54, 133.37, 133.95, 136.49, 138.39, 141.77, 142.28, 142.92, 143.31, 144.18, 146.85, 148.65, 156.23, 156.40, 156.48, 156.51, 166.62. ESI-MS (*m/z*): $[M+4CF_3COO]^{2+}$calcd. for $C_{106}H_{88}F_{12}N_{18}O_{16}Zn^{2+}$ 1080.28; found 1080.47.

Compound 4 [37]

4-Hydroxybenzaldehyde (1 g, 8.2 mmol) and ethyl 4-bromobutyrate (1.6 g, 8.2 mmol) were dissolved in 10 mL DMF in presence of K_2CO_3 (2.3 g, 16.4 mmol) and the system was heated to 70 °C for 6 hours. After that, the solution was diluted with ethyl acetate and washed with water (50 mL × 3), and the organic phase was concentrated and loaded onto a silica column with EA/n-hexane (1/5) as elute to give product **4** (1.5 g, 79%). . ^{1}H NMR (400 MHz, $CDCl_3$) δ (ppm): 1.28 (3H, t, J = 7.16 Hz), 2.17 (2H, m, J = 6.64 Hz), 2.55 (2H, t, J = 7.16 Hz), 4.13 (4H, m), 7.01 (2H, d, J = 8.76 Hz), 7.85 (2H, d, J = 8.76 Hz), 9.90 (1H, s). ^{13}C NMR (100 MHz, $CDCl_3$) δ (ppm): 14.21, 24.41, 30.59, 60.52, 67.13, 114.74, 129.97, 131.96, 163.87, 172.94, 190.73.

Porphyrin 7 [37]

Then a mixture of compound **4** (1.25 g, 5.3 mmol), 4-pyridinecarboxaldehyde (1.7 g, 15.9 mmol) and propionic acid (100 mL) was heated at 110 °C with stirring. To this solution pyrrole (1.4 g, 21.2 mmol) was added dropwise and the resulting mixture was refluxed for 2 h. After reaction propionic acid was removed under vacuum and the residue was purified using a silica column with EtOH/DCM = 1/50 as elute, finally giving 278 mg porphyrin **7** (7% yield). ^{1}H NMR (400 MHz, $CDCl_3$) δ (ppm): 1.37 (3H, t, J = 7.12 Hz), 2.35 (2H, m, J = 6.68 Hz), 2.73 (2H, t, J = 7.24 Hz), 4.27 (2H, q, J = 7.08 Hz), 4.35 (2H, t, J = 6.04 Hz), 7.32 (2H, d, J = 10.28 Hz), 8.13 (2H, d, J = 8.44 Hz), 8.19 (6H, d, J = 4.56 Hz), 8.84 (2H, d, J = 4.80 Hz), 8.88 (4H, s), 8.98 (2H, d, J = 4.84 Hz), 9.08 (6H, d, J = 5.92 Hz). ^{13}C NMR (100 MHz, $CDCl_3$) δ (ppm): 14.34, 24.87, 30.98, 60.59, 67.14, 112.96, 116.90, 117.40, 121.73, 129.37, 133.88, 135.68, 148.39, 148.43, 149.99, 150.06, 159.04, 173.31. Symmetrical porphyrin **8** was purified from the mixture as one side product. ^{1}H NMR (400 MHz, $CDCl_3$) δ (ppm): 8.19 (8H, d, J = 4.84 Hz), 8.90 (8H, s), 9.09 (8H, d, J = 5.12 Hz).

Sym-ZnPorp [52]

Porphyrin **8** (100 mg, 0.16 mmol) was dissolved in 10 mL dry DMF and then mixed with 1 mL iodomethane in a sealed bottle, afterwards the mixture was heated to 40 °C overnight. The separation was conducted on a reverse phase HPLC system and the separated product was given as sym-Porp. ^{1}H NMR (400 MHz, DMSO-d_6) δ 4.74 (12H, s), 8.99 (8H, d, J = 6.56 Hz), 9.18 (8H, s), 9.49 (8H, d, J = 6.24 Hz). ESI-MS (m/z): $[M-H]^{3+}$ calcd. for $C_{44}H_{37}N_8$ 225.67; found 225.85. The coordination of Zn (II) was conducted by stirring sym-Porp with 2 equivalent $Zn(OAc)_2$ in EtOH overnight, and the given product was separated using reverse phase HPLC and freeze dried as sym-ZnPorp. ESI-MS (m/z): $[M-H]^{3+}$ calcd. for $C_{44}H_{35}N_8Zn$ 246.75; found 246.49.

ZnPorpCur and ZnPorpBex

100 mg porphyrin **7** was dissolved in a mixture of 15 mL dioxane and 4 mL MeOH, and afterwards 2 mL NaOH solution (2 N) was added.

The mixture was further stirred for 1 hour and then 5 mL hydrochloric acid (1 N) was added, and the product was precipitated out by adding saturated $NaHCO_3$ solution. The collected solid was dried under vacuum and used directly for next step.

The deprotected porphyrin (50 mg, 0.07 mmol) was mixed with EDC (40 mg, 0.21 mmol) and HoBt (28 mg, 0.21 mmol) in 5 mL DMF, and then amino-curcumin or amino-bexarotene(0.07 mmol) was added to the mixture together with DIEA (37 µL, 0.21 mmol), which was followed by overnight stirring under nitrogen. The solvent was then evaporated and the product was separated using a silica column with EtOH/DCM = 1/50 as eluent. The collected solid was dissolved in 5 mL dry DMF in a 15 mL sealed bottle and then 1 mL iodomethane was added. Then mixture was heated to 40 °C overnight, and then by using a reverse phase HPLC system could the final product be acquired as metal free Porp-Cur or Porp-Bex.

Porp-Cur. ^{1}H NMR (400 MHz, DMSO-d_6) δ (ppm): 1.97 (2H, t, J = 6.32 Hz), 2.19 (2H, s), 2.47 (2H, m), 3.33 (2H, d, J = 6.28 Hz), 3.80 (3H, s), 3.86 (3H, s), 4.10 (2H, s), 4.31 (2H, s), 4.76 (9H, s), 5.87 (1H, s), 6.54 (1H, d, J = 15.84 Hz), 6.68 (1H, d, J = 15.92 Hz), 6.78 (1H, d, J = 8.08 Hz), 7.01 (2H, d, J = 7.24 Hz), 7.19 (2H, s), 7.42 (5H, m), 8.15 (3H, m), 9.02 (14H, m), 9.52 (6H, m). ^{13}C NMR (100 MHz, DMSO-d_6) δ (ppm): 25.53, 29.22, 32.29, 36.13, 48.39, 56.08, 56.13, 66.72, 67.77, 101.13, 111.02, 111.51, 112.68, 113.08, 113.69, 114.63, 115.57, 115.63, 115.93, 118.57, 121.26, 121.52, 122.24, 123.26, 123.36, 123.52, 126.56, 128.00, 132.63, 132.91, 136.14, 140.22, 140.92, 144.59, 148.24, 149.52, 149.55, 150.59, 157.10, 157.21, 159.37, 172.44, 182.17, 183.26. ESI-MS (m/z): $[M-H]^{3+}$ calcd. for $C_{72}H_{66}N_8O_8^{3+}$ 390.17; found 390.34.

Porp-Bex. ^{1}H NMR (400 MHz, DMSO-d_6) δ (ppm): 0.97 (6H, s), 1.08 (6H, s), 1.78 (3H, s), 2.13 (2H, m), 2.42 (2H, t, J = 7.28 Hz), 3.32 (2H, m), 3.40 (2H, m), 4.23 (2H, t, J = 6.48 Hz), 4.70 (9H, s), 5.07 (1H, s), 5.78 (1H, s), 6.87 (1H, s), 6.98 (1H, s), 7.26 (2H, d, J = 8.08 Hz), 7.36 (2H, d, J = 8.12 Hz), 7.80 (2H, d, J = 8.16 Hz), 8.07 (2H, d, J = 6.28 Hz), 8.93 (6H, d, J = 6.00 Hz), 9.38 (6H, d, J = 6.04 Hz). ^{13}C NMR (100 MHz, DMSO-d_6) δ (ppm): 19.78, 25.42, 31.81, 31.85, 32.29, 33.66, 33.87, 34.86, 48.43, 67.66, 113.69, 114.59, 115.52, 117.01, 118.46, 121.41, 123.57, 126.48, 127.55, 127.90, 128.17, 132.44, 132.63, 132.80, 133.74, 136.07, 138.19, 142.21, 143.39, 144.14, 144.51, 148.45, 157.13, 158.68, 159.02, 159.30, 166.94, 173.11. ESI-MS (m/z): $[M-H]^{3+}$ calcd. for $C_{74}H_{73}N_9O_3$ 378.53; found 378.83.

The chelation of zinc (II) ion was conducted in ethanol, where 1 equivalent metal free Porp-Cur or Porp-Bex was mixed with 2 equivalent $Zn(OAc)_2$, and then the mixture was stirred at room temperature overnight. Afterwards, the mixture was separated using reverse phase HPLC to acquire the final product, *i.e.* ZnPorpCur or ZnPorpBex. The collected portions were freeze dried and the metal contents were determined using an ICP-OES before usage.

Peptide preparation

The purchased $A\beta_{42}$ peptide was treated according to the previous reports. [53, 54] Firstly, the lyophilized $A\beta_{42}$ peptide was dissolved in 1,1,1,3,3,3-hexafluoro-2-isopropanol (HFIP, Sigma-Aldrich) to give a concentration of 2 mg/mL, which was followed by incubation of 2 hours at 37 °C. After that, nitrogen flow was used to dry HFIP to give $A\beta_{42}$ film on the surface of the bottle. This process was repeated for 3 times to disaggregate $A\beta_{42}$ and the finally resulted $A\beta_{42}$ film was dried under vacuum overnight and then stored at -20 °C until further usage. The pretreated $A\beta_{42}$ film was dissolved in 6 mM NaOH solution at a concentration of 0.5 mM as stocks for incubation study.

ThT assay

Thioflavin T (ThT) was purchased from Sigma-Aldrich and prepared as 1 mM stock in water. The pretreated $A\beta_{42}$ film in 6 mM NaOH solution was diluted to 10 µM using incubation buffer (20 mM sodium phosphate, 272 mM NaCl, pH 7.4) in presence of 20 µM ThT. For dose dependent inhibition study, the investigated compounds such as porphyrin analogues and phthalocyanine analogues were prepared as 1 mM stock solutions in water and then diluted into the incubation system at various concentrations, *i.e.* 0.001, 0.003, 0.01, 0.03, 0.1, 0.3, 1, 3 and 10 µM. The incubated mixtures were seeded into a 96 well plate and incubated for 24 hours and 48 hours respectively before monitoring the fluorescence intensity of ThT using a multimode microplate reader (BMG LABTECH CLARIOstar, λ_{ex} = 445 nm and λ_{em} = 480 nm). The acquired data were analyzed using GraphPad Prism to obtain IC_{50} values using log (concentration) *vs.* normalized response-variable slope. The fluorescence emission spectra of ThT incubated with Aβ species were recorded using an Edinburgh Instruments FLSP920 spectrophotometer equipped with a Xe900 continuous xenon lamp (450 W), with excitation wavelength fixed at 440 nm and excitation wavelength collected from 450 to 600 nm.

Circular dichroism

0.5 mM stock of $A\beta_{42}$ peptide in 6 mM NaOH solution was diluted into 20 mM phosphate buffer containing 272 mM NaCl, pH 7.4 to acquire a 10 µM solution. Porphyrin and Pc analogues were diluted from the stocks to desired concentrations and then co-incubated with $A\beta_{42}$ peptide at 37 °C for 48 hours before examination. The CD

spectra were recorded at 1 nm intervals from 200 to 260 nm with scanning speed at 100 nm every minute on a Jasco J-1500 CD spectropolarimeter.

Western blot analysis

Western blot was used to analyze the aggregation states of incubated $A\beta_{42}$ peptide in presence or absence of various compounds. $A\beta_{42}$ samples (5 μL, 10 μM) was mixed with 2 μL Laemmli sample buffer (Bio-Rad) and loaded onto 4-15% Mini-PROTEAN TGX gel (Bio-Rad) for SDS-PAGE using Tris/glycine running buffer. Afterwards, the protein bands were transferred to PVDF membrane using a standard method for 30 min at room temperature. The membrane was blocked with 5% nonfat milk in Tris-buffered saline (TBST, 25 mM Tris, 150 mM NaCl, pH 7.4, containing 0.05% Tween 20) for 1 hour at room temperature, which was followed by incubation with polyclonal Aβ antibody (Cell signaling, primary antibody, 1:2000 dilution) overnight at 4 °C. Following the washing with TBST (3 × 5 min), the membrane was probed with anti-rabbit IgG, HRP-linked Antibody (1:4000, Cell signaling) for 1 hour at room temperature. Then the blot was washed with TBST (3 × 5 min) and protein were viewed under a Bio-rad ChemiDoc MP imaging system.

Transmission electron microscopy

$A\beta_{42}$ peptide was incubated in buffer (20 mM phosphate, 272 mM NaCl, pH 7.4) at a concentration of 10 μM with various compounds respectively for 48 hours. Then 5 μL of each sample was applied to carbon-coated copper TEM grids (300 mesh) for 30 min at room temperature. Afterwards, excess liquid was removed with filter paper and washed with 5 μL water for 10 s before staining with uranyl acetate (2%, w/v) for 20 s. Copper girds were viewed with a Field Emission Electron Microscope STEM (JEOL Model JEM-2100F) operated at 200 kV, equipped with a high resolution CCD camera.

MTT assay

Human cervical cancer HeLa cells were grown in Dulbecco's Modified Eagle Medium (DMEM). About 5×10^3 cells per well in the culture medium were inoculated in 96-multiwell plates and incubated overnight at 37 °C in a humidified 5% CO_2 atmosphere. ZnPc/porphyrin analogues were dissolved in phosphate buffered saline (PBS) to give 10 mM solutions, which were diluted to various concentrations with the culture mediums. For dark toxicity study, the cells were firstly rinsed with PBS, and then were incubated with 100 μL of the diluted compounds solutions (5, 10, 20, 30, 50, 100 μM) for 24 h at 37 °C under 5% CO_2. Afterwards, the cells were then rinsed again with PBS and refed with 100 μL of the culture medium containing MTT (0.5 mg/mL) followed by incubation for 4 hours at the same environment. After that, solutions were removed from each hole and 100 μL DMSO was added to dissolve the formed crystal before measurement of the absorption at 490 nm. The recorded values reflected the viability of cells by comparing to the groups in absence of extra compounds.

Conflicts of interest

There are no conflicts to declare.

Acknowledgements

G.-L. L gratefully acknowledge the Research Grants Council of Hong Kong (15300919, PolyU 153103/16P, PolyU 153014/15P), the State Key Laboratory of Chemical Biology and Drug Discovery, the Hong Kong Polytechnic University ((a) University Research Facility in Chemical and Environmental Analysis (UCEA); (b) University Research Facility in Life Sciences (ULS)). HKBU Inter-institutional Collaborative Research Scheme (RC-ICRS/1617/02A-BOL to H.L.L.), and seed money from Faculty of Science of HKBU to new academic staff (Project title: Translational and Molecular Cancer Science to H.L.L.).

Notes and references

1 M. Citron, *Nat. Rev. Drug Discov.*, 2010, **9**, 387.
2 R. Limbocker, S. Chia, F.S. Ruggeri, M. Perni, R. Cascella, G.T. Heller, G. Meisl, B. Mannini, J. Habchi, T.C.T. Michaels, P.K. Challa, M. Ahn, S.T. Casford, N. Fernando, C.K. Xu, N.D. Kloss, S.I.A. Cohen, J.R. Kumita, C. Cecchi, M. Zasloff, S. Linse, T.P.J. Knowles, F. Chiti, M. Vendruscolo, C.M. Dobson, *Nat. Commun.*, 2019, **10**, 225.
3 S. Lee, X. Zheng, J. Krishnamoorthy, M.G. Savelieff, H.M. Park, J.R. Brender, J.H. Kim, J.S. Derrick, A. Kochi, H.J. Lee, C. Kim, A. Ramamoorthy, M.T. Bowers, M.H. Lim, *J. Am. Chem. Soc.*, 2014, **136**, 299.
4 A.K. Sharma, S.T. Pavlova, J. Kim, D. Finkelstein, N.J. Hawco, N.P. Rath, J. Kim, L.M. Mirica, *J. Am. Chem. Soc.*, 2012, **134**, 6625.
5 S. De, D.C. Wirthensohn, P. Flagmeier, C. Hughes, F.A. Aprile, F.S. Ruggeri, D.R. Whiten, D. Emin, Z. Xia, J.A. Varela, P. Sormanni, F. Kundel, T.P.J. Knowles, C.M. Dobson, C. Bryant, M. Vendruscolo, D. Klenerman, *Nat. Commun.*, 2019, **10**, 1541.
6 C. Haass, D.J. Selkoe, *Nat. Rev. Mol.*, 2007, **8**, 101.
7 D.J. Selkoe, J. Hardy, *EMBO Mol. Med.*, 2016, **8**, 595.
8 F. Chiti, C.M. Dobson, *Annu. Rev. Biochem.*, 2017, **86**, 27.
9 T.P.J. Knowles, M. Vendruscolo, C.M. Dobson, *Nat. Rev. Mol.*, 2014, **15**, 384.
10 W.S. Caughey, L.D. Raymond, M. Horiuchi, B. Caughey, *Proc. Natl. Acad. Sci.*, 1998, **95**, 12117.
11 S.A. Priola, A. Raines, W.S. Caughey, *Science*, 2000, **287**, 1503.
12 W.S. Caughey, S.A. Priola, D.A. Kocisko, L.D. Raymond, A. Ward, B. Caughey, *Antimicrob. Agents Chemother.*, 2007, **51**, 3887.

13 G.R. Lamberto, A. Binolfi, M.L. Orcellet, C.W. Bertoncini, M. Zweckstetter, C. Griesinger, C.O. Fernandez, *Proc. Natl. Acad. Sci.*, 2009, **106**, 21057.
14 E.N. Lee, H.J. Cho, C.H. Lee, D. Lee, K.C. Chung, S.R. Paik, *Biochemistry*, 2004, **43**, 3704.
15 S. Taniguchi, N. Suzuki, M. Masuda, S. Hisanaga, T. Iwatsubo, M. Goedert, M. Hasegawa, *J. Biol. Chem.*, 2005, **280**, 7614.
16 E. Akoury, M. Gajda, M. Pickhardt, J. Biernat, P. Soraya, C. Griesinger, E. Mandelkow, M. Zweckstetter, *J. Am. Chem. Soc.*, 2013, **135**, 2853.
17 A.A. Valiente-Gabioud, D. Riedel, T.F. Outeiro, M.A. Menacho-Márquez, C. Griesinger, C.O. Fernández, *Biophys. J.*, 2018, **114**, 1036.
18 S. Tabassum, A.M. Sheikh, S. Yano, T. Ikeue, M. Handa, A. Nagai, *FEBS J*, 2015, **282**, 463.
19 A.A. Valiente-Gabioud, M.C. Miotto, M.E. Chesta, V. Lombardo, A. Binolfi, C.O. Fernández, *Acc. Chem. Res.*, 2016, **49**, 801.
20 C. Jing, R. Wang, H. Ou, A. Li, Y. An, S. Guo, L. Shi, *Chem. Commun.*, 2018, **54**, 3985.
21 X. Li, S. Yu, Y. Lee, T. Guo, N. Kwon, D. Lee, S.C. Yeom, Y. Cho, G. Kim, J.-D. Huang, S. Choi, K.T. Nam, J. Yoon, *J. Am. Chem. Soc.*, 2019, **141**, 1366.
22 X. Zhao, Y. Huang, G. Yuan, K. Zuo, Y. Huang, J. Chen, J. Li, J. Xue, *Chem. Commun.*, 2019, **55**, 866.
23 H. Yaku, T. Fujimoto, T. Murashima, D. Miyoshi, N. Sugimoto, *Chem. Commun.*, 2012, **48**, 6203.
24 J.W. Park, J.S. Ahn, J.H. Lee, G. Bhak, S. Jung, S.R. Paik, *Chembiochem*, 2008, **9**, 2602.
25 Y. Fan, D. Wu, X. Yi, H. Tang, L. Wu, Y. Xia, Z. Wang, Q. Liu, Z. Zhou, J. Wang, *ACS Omega*, 2017, **2**, 4188.
26 N. Kokkoni, K. Stott, H. Amijee, J.M. Mason, A.J. Doig, *Biochemistry*, 2006, **45**, 9906.
27 L.O. Tjernberg, J. Naslund, F. Lindqvist, J. Johansson, A.R. Karlstrom, J. Thyberg, L. Terenius, C. Nordstedt, *J. Biol. Chem.*, 1996, **271**, 8545.
28 A. Hirabayashi, Y. Shindo, K. Oka, D. Takahashi, K. Toshima, *Chem. Commun.*, 2014, **50**, 9543.
29 V. Villari, R. Tosto, G. Di Natale, A. Sinopoli, M.F. Tomasello, S. Lazzaro, N. Micali, G. Pappalardo, *ChemistrySelect*, 2017, **2**, 9122.
30 Q. Zhan, X. Shi, T. Wang, J. Hu, J. Zhou, L. Zhou, S. Wei, *Talanta*, 2019, **191**, 27.
31 T. Mohamed, A. Shakeri, G. Tin, P.P.N. Rao, *ACS Med. Chem. Lett.*, 2016, **7**, 502.
32 R.M.C. Di Martino, A. De Simone, V. Andrisano, P. Bisignano, A. Bisi, S. Gobbi, A. Rampa, R. Fato, C. Bergamini, D.I. Perez, A. Martinez, G. Bottegoni, A. Cavalli, F. Belluti, *J. Med. Chem.*, 2016, **59**, 531.
33 A. Thapa, S.D. Jett, E.Y. Chi, *ACS Chem. Neurosci.*, 2016, **7**, 56.
34 Y. Masuda, M. Fukuchi, T. Yatagawa, M. Tada, K. Takeda, K. Irie, K.-i. Akagi, Y. Monobe, T. Imazawa, K. Takegoshi, *Bioorg. Med. Chem.*, 2011, **19**, 5967.
35 P.E. Cramer, J.R. Cirrito, D.W. Wesson, C.Y.D. Lee, J.C. Karlo, A.E. Zinn, B.T. Casali, J.L. Restivo, W.D. Goebel, M.J. James, K.R. Brunden, D.A. Wilson, G.E. Landreth, *Science*, 2012, **335**, 1503.
36 P.D.Q. Huy, N.Q. Thai, Z. Bednarikova, L.H. Phuc, H.Q. Linh, Z. Gazova, M.S. Li, *ACS Chem. Neurosci.*, 2017, **8**, 1960.
37 M. Marketaki, E. Touloupakis, G. Charalambidis, M.-C. Chalbot, D.F. Ghanotakis, A.G. Coutsolelos, *J. Porphyr. Phthalocya.*, 2012, **16**, 997.
38 M. Sasaki, Y. Ryoson, M. Numata, G. Fukuhara, *J. Org. Chem.*, 2019, **84**, 6017.
39 K. Groves, A.J. Wilson, A.D. Hamilton, *J. Am. Chem. Soc.*, 2004, **126**, 12833.
40 F. Giuntini, F. Foglietta, A.M. Marucco, A. Troia, N.V. Dezhkunov, A. Pozzoli, G. Durando, I. Fenoglio, L. Serpe, R. Canaparo, *Free Radic. Biol. Med.*, 2018, **121**, 190.
41 A.G. Kreutzer, S. Yoo, R.K. Spencer, J.S. Nowick, *J. Am. Chem. Soc.*, 2017, **139**, 966.
42 S.S.S. Wang, Y.T. Chen, S.W. Chou, *Biochim. Biophys. Acta Mol. Basis Dis.*, 2005, **1741**, 307.
43 S.A. Hudson, H. Ecroyd, T.W. Kee, J.A. Carver, *FEBS J.*, 2009, **276**, 5960.
44 S.G. Bolder, L.M.C. Sagis, P. Venema, E. van der Linden, *Langmuir*, 2007, **23**, 4144.
45 T. Shi, M. Wang, H. Li, M. Wang, X. Luo, Y. Huang, H.H. Wang, Z. Nie, S. Yao, *Sci. Rep.*, 2018, **8**, 5551.
46 S. Lee, X. Zheng, J. Krishnamoorthy, M.G. Savelieff, H.M. Park, J.R. Brender, J.H. Kim, J.S. Derrick, A. Kochi, H.J. Lee, C. Kim, A. Ramamoorthy, M.T. Bowers, M.H. Lim, *J. Am. Chem. Soc.*, 2014, **136**, 299.
47 A.K. Sharma, S.T. Pavlova, J. Kim, D. Finkelstein, N.J. Hawco, N.P. Rath, J. Kim, L.M. Mirica, *J. Am. Chem. Soc.*, 2012, **134**, 6625.
48 M.R. Jones, E. Mathieu, C. Dyrager, S. Faissner, Z. Vaillancourt, K.J. Korshavn, M.H. Lim, A. Ramamoorthy, V. Wee Yong, S. Tsutsui, P.K. Stys, T. Storr, *Chem. Sci.*, 2017, **8**, 5636.
49 M.W. Beck, J.S. Derrick, R.A. Kerr, S.B. Oh, W.J. Cho, S.J. Lee, Y. Ji, J. Han, Z.A. Tehrani, N. Suh, S. Kim, S.D. Larsen, K.S. Kim, J.Y. Lee, B.T. Ruotolo, M.H. Lim, *Nat. Commun.*, 2016, **7**, 13115.
50 X. Zhang, Y. Tian, Z. Li, X. Tian, H. Sun, H. Liu, A. Moore, C. Ran, Journal of the American Chemical Society, 135 (2013) 16397-16409.
51 Y. Porat, A. Abramowitz, E. Gazit, *Chem. Biol. Drug Des.*, 2006, **67**, 27.
52 M. Saghian, S. Dehghanpour, M. Sharbatdaran, *New J. Chem.*, 2018, **42**, 12872.
53 J. Hatai, L. Motiei, D. Margulies, *J. Am. Chem. Soc.*, 2017, **139** 2136.
54 D. Shea, C.C. Hsu, T.M. Bi, N. Paranjapye, M.C. Childers, J. Cochran, C.P. Tomberlin, L. Wang, D. Paris, J. Zonderman, G. Varani, C.D. Link, M. Mullan, V. Daggett, *Proc. Natl. Acad. Sci.*, 2019, **116**, 8895.